Transcriptome sequencing reveals genes involved in cadmium-triggered oxidative stress in the chicken heart

Chunlin Yu,[*,†,1] Mohan Qiu,[*,†,1] Zengrong Zhang,[*,†] Xiaoyan Song,[*,†] Huarui Du,[*,†] Han Peng,[*,†] Qingyun Li,[*,†] Li Yang,[*,†] Xia Xiong,[*,†] Bo Xia,[*,†] Chenming Hu,[*,†] Jialei Chen,[*,†] Xiaosong Jiang,[*,†] and Chaowu Yang[*,†,2]

*Sichuan Animal Science Academy, Chengdu, Sichuan 610066 China; and †Animal Breeding and Genetics Key Laboratory of Sichuan Province, Chengdu, Sichuan 610066 China

ABSTRACT As a ubiquitous heavy metal, cadmium (**Cd**) is highly toxic to various organs. However, the effects and molecular mechanism of Cd toxicity in the chicken heart remain largely unknown. The goal of our study was to investigate the cardiac injury in chickens' exposure to Cd. We detected the levels of oxidative stress–related molecules in the Cd-induced chicken heart, and assessed the histopathological changes by hematoxylin and eosin staining. RNA sequencing was performed to identify differentially expressed mRNAs between the Cd-induced group and control group. The expression of candidate genes involved in oxidative stress was certified by quantitative reverse transcription PCR. Our results showed that the expression of glutathione, peroxidase, and superoxide dismutase was significantly decreased and malondialdehyde was increased in the heart of chickens by Cd induction. The disorderly arranged cardiomyocytes, swelled and enlarged cells, partial cardiomyocyte necrosis, blurred morphological structure, and notable inflammatory cell infiltration were observed in the Cd-induced chicken heart. RNA sequencing identified 23 upregulated and 11 downregulated mRNAs in the heart tissues of the chicken in the Cd-induced group, and functional pathways indicated that they were associated with oxidative stress. Moreover, CREM, DUSP8, and ITGA11 expressions were significantly reduced, whereas LAMA1 expression was induced in heart tissue of chickens by Cd treatment. Overall, our findings revealed that oxidative stress and pathological changes in the chicken heart could be triggered by Cd. The mRNA transcriptional profiles identified differentially expressed genes in the chicken heart by Cd induction, revealing oxidative stress–related key genes and enhancing our understanding of Cd toxicity in the chicken heart.

Key words: oxidative stress, cadmium, toxicity, mRNA

2021 Poultry Science 100:100932
https://doi.org/10.1016/j.psj.2020.12.029

INTRODUCTION

Cadmium (**Cd**) is a highly toxic metal that is extensively present in the environment, which has a long elimination half-life, and its residual in the food chain seriously threatens human health (Ezedom and Asagba, 2016). Because Cd possesses the same charge, a similar ionic radius, and similar chemical behaviors to calcium, Cd can enter the body and accumulate to high levels in multiple organs (Kubier et al., 2019). It has been reported that Cd toxicity can induce oxidative damage, inflammatory response, and morphological damage, which in turn initiate various diseases (Wang et al., 2008; Liu et al., 2015; Zhang et al., 2017). Recent research showed that Cd pollution was detected in food, especially in meat and offal (Nouri and Haddioui, 2016). As an important source of meat, chicken contains enriched vitamins, fibers, essential amino acids, and minerals (Tang et al., 2019). Therefore, it is of great significance to study the toxicological mechanism of Cd in chickens.

Several studies demonstrated that Cd posed toxic threat to the health of humans and animals, including that of chickens. Cytotoxicity, including nucleus

Received June 5, 2020.
Accepted December 15, 2020.

[1]Equal contributors.

[2]Corresponding author: cwyang@foxmail.com

damage, morphological abnormalities, antioxidant depletion, and increased apoptosis rate, could be observed in Cd-treated chicken erythrocytes (Zhang et al., 2018a). BNIP3-mediated autophagy and BNIP3-impairing ion homeostasis could be triggered in the spleen of chickens under Cd treatment (Zhang et al., 2018a). Cadmium exposure enhanced the concentration of Cd in the chicken kidneys, resulting in denaturation and necrosis of renal tubular epithelial cells and narrowing or disappearance of tubules (Wang et al., 2017). Cadmium mediated the apoptosis of hepatocytes in chickens via changing heat shock protein–related genes, apoptosis-related genes, and P13 K/AKT pathway–related genes (Xiong et al., 2019). Cadmium induction contributed to cardiac abnormal functions and histopathology changes as well as increased nitric oxide synthase activities and cardiac inflammation through facilitation of the expression of inflammation factors (Guo et al., 2020). However, the function and mechanism of Cd induction in the chicken heart remain unclear.

Evidence strongly revealed that oxidative stress played a key role in Cd-mediated tissue damage and cytotoxicity, which was considered as one of the major mechanisms of this cytotoxicity (Tang et al., 2019). The quality of chicken breast meat could be declined by Cd via oxidative stress and inflammation (Tang et al., 2019). Cadmium triggered oxidative stress and mitochondrial dysfunction in the chicken kidney by suppressing the unfolded protein response expression level and activating Nrf2-mediated antioxidant defense (Ge et al., 2019). The accumulation of Cd induced apoptosis and oxidative stress in the chicken spleen by increasing the content of malondialdehyde (**MDA**) and inflammatory factors, activating antioxidant enzymes (superoxide dismutase **[SOD]**, glutathione peroxidase), and promoting increase in apoptotic protein (Bcl-2, caspase-3, Bax) levels (Teng et al., 2019). Cadmium initiated inflammatory damage and oxidant stress in chicken livers (Hu et al., 2017). Moreover, Cd treatment could induce oxidative stress in the heart of chickens by activating the Nrf2 signaling pathway via mounting the expression of pivotal target genes (GCLC, HO-1, SOD, GCLM, NQO1) (Guo et al., 2020). Nevertheless, the biomolecule and transcriptional dynamics in the chicken heart's response to Cd have not been reported.

This study aimed to elucidate cardiac damage and suggest the regulation mechanism of oxidative stress in chickens subjected to Cd induction. The levels of oxidative stress–related molecules were detected in the heart tissues of chickens subjected to Cd induction, and hematoxylin and eosin (**H&E**) staining was used to evaluate the pathological changes of the chicken heart. Moreover, high-throughput sequencing of chicken heart tissues was performed to explore the crucial genes involved in oxidative stress during cardiac damage triggered by Cd. Quantitative real-time PCR (**RT-qPCR**) was used to evaluate the expression levels of crucial genes in the heart tissues of chickens.

MATERIALS AND METHODS

Animals and Treatments

Forty male healthy broilers (7-day-old) were randomized to 2 groups (20 broilers per group). The Cd group received the basal diet supplemented with 140 mg/kg of cadmium chloride ($CdCl_2$,Cd; C116344; Sigma, Aladdin Chemical Co., Ltd, Shanghai, China), whereas the control group was given solely a basal diet (Xu et al., 2017; Yu et al., 2020). The composition and nutrient level of the basal diet are presented in Table 1. The broilers in the 2 groups were given free access to water and food during the entire experimental process. At day 20, 40, and 60, five broilers from every group were randomly screened for euthanasia, and the heart tissues were collected and divided into 4 parts. Three parts for oxidative stress detection, transcriptome sequencing, and PCR detection were stored at −70°C, whereas the other part was fixed in paraformaldehyde and embedded in paraffin for histopathological observation. All treatment procedures were approved by the Institutional Animal Care and Use Committee of Sichuan Animal Science Academy.

Measurement of Oxidative Stress–Related Molecules

The heart tissues were homogenized with physiological saline in freezing tubes and then centrifuged for 10 min at 3,000 rpm to collect the supernatant. The level of reduced glutathione (**GSH**) in chicken heart tissues was detected using a glutathione assay kit (BC1170; Beijing Solarbio Science & Technology Co., Ltd., Beijing, China) as follows: fresh tissues were put in the

Table 1. Composition and nutrient levels of basal diet for broilers.

Ingredient (%)	Starter (1–28 d)	Finisher (29–75 d)
Corn	59.80	67.00
Soybean meal	11.20	10.00
Corn germ meal	14.30	8.70
Corn gluten meal	8.00	8.00
Fish meal	2.00	2.00
Sodium chloride	0.29	0.29
Limestone	1.25	1.20
Calcium hydrogen phosphate	1.85	1.60
L-Lysine	0.46	0.42
DL-Methionine	0.14	0.08
Antioxidant	0.01	0.01
Premix[a]	0.70	0.70
Total	100.00	100.00
Nutrition value		
ME (MJ/kg)	11.93	12.35
Protein (%)	19.14	18.02
Calcium (%)	1.01	0.92
Total phosphorus (%)	0.47	0.42
Lysine (%)	1.10	0.99
Methionine (%)	0.48	0.41

[a]Premix (0.7%) provides the following per kilogram of diet: vitamin A, 6000 international unit (IU); vitamin D3, 1500 IU; vitamin E, 20 IU; vitamin B12, 0.01 mg; vitamin K3, 0.7 mg; folic acid, 0.6 mg; nicotinic acid, 40 mg; pantothenic acid, 9 mg; biotin, 0.2 mg; and pyridoxine, 2.2 mg. Mineral premix contained the following per kilogram of diet: Fe, 80 g; Cu, 7 mg; Zn, 80 mg; Mn, 100 mg; I, 0.5 mg; and Se, 0.2 mg.

homogenizer, which was rinsed with reagent 1; reagent 1 was added (tissue-to-reagent ratio remained unchanged), and the resultant was quickly ground on ice and centrifuged at 8,000× *g* for 10 min at 4°C; the supernatant was stored at 4°C until assayed; standard curves were generated using the pure standard; 20 μL of the sample, 140 μL of reagent 2, and 40 μL of reagent 3 were successively added to a 96-well plate and then incubated for 2 min; the absorbance was detected at 412 nm using a microplate reader (Infinite M1000; TECAN, Männedorf, Switzerland); and GSH content was calculated based on the manufacturer's formula. This experiment has two independent samples at each time point, including the Cd treatment sample and the control sample, and each of the samples at each time point had five biology repeats.

The lipid peroxidation level was tested using the lipid peroxidation MDA assay kit (S0131; Shanghai Biyuntian Biotechnology Co., Ltd., Shanghai, China) as follows: tissues was homogenized by RIPA lysis solution (Biyuntian Biotechnology Co., Ltd., Shanghai, China) and centrifuged for 10 min at 10,000–20,000× *g*, and the supernatant was removed; standard curves were generated; 0.1 mL of tissue homogenates was placed into the centrifuge tube, mixed with 0.2 mL of MDA working buffer, and heated in a boiling water for 15 min, and the resultant was left to cool to room temperature and centrifuged at 1,000× *g* for 10 min; 200 μL of the supernatant was used to measure the absorbance at 532 nm; and the MDA content was calculated based on the manufacturer's instructions. This experiment has two independent samples at each time point, including the Cd treatment sample and the control sample, and each of the samples at each time point had five biology repeats.

The activity of SOD was detected using the superoxide dismutase assay kit (BC0175; Beijing Solarbio Science & Technology Co., Ltd., Beijing, China) as follows: tissues (0.05 g) were mixed with extract (0.5 mL), homogenized, and centrifuged at 8,000× *g* for 10 min at 4°C; the supernatant was removed and placed on ice; 18 μL of the supernatant, 45 μL of reagent 1, 2 μL of reagent 2, 35 μL of reagent 3, 10 μL of reagent 5, and 90 μL of water were successively added to a 96-well plate; the absorbance value at 560 nm was recorded; and SOD activity was calculated according to the manufacturer's instructions. This experiment has two independent samples at each time point, including the Cd treatment sample and the control sample, and each of the samples at each time point had five biology repeats.

The activity level of peroxidase (**POD**) was detected using the peroxidase assay kit (BC0090; Beijing Solarbio Science & Technology Co., Ltd., Beijing, China) as follows: tissues (0.05 g) were mixed with extract (0.5 mL), homogenized, and centrifuged at 8,000× *g* for 10 min at 4°C; the supernatant was removed and placed on ice, 3 μL of supernatant; 54 μL of water, 104 μL of reagent 1, 26 μL of reagent 2, and 27 μL of reagent 3 were successively added to a 96-well plate; the absorbance value A1 at 470 nm was recorded at 30 s, and the absorbance value A2 was recorded after 1 min ($\Delta A = A1 - A2$); and POD activity was calculated according to the manufacturer's instructions. This experiment has 2 independent samples at each time point, including the Cd treatment sample and the control sample, and each of the samples at each time point had 5 biology repeats.

Histopathological Examination of the Chicken Heart

The pathological changes in the chicken heart (60 d) were evaluated by routine H&E staining. In brief, paraffin sections were dewaxed in water, cell nuclei were counterstained with hematoxylin, and cytoplasm was stained with eosin. Finally, the sections were dehydrated in ethanol gradient and diaphanized, and the slides were sealed with neutral balsam. The pathological changes in the chicken heart were observed using a light microscope. Two independent samples (Cd treatment sample and control sample) on day 60 were used in this experiment. Each of the samples had four biology repeats.

RNA Isolation and Transcriptome Sequencing

RNA in the chicken heart was extracted using the TRIZOL reagent (15596026; Invitrogen; Thermo Fisher Scientific, Inc., Shanghai, China), and its quantity and purity was measured using the NanoDrop ONE (NDONEC-W; Thermo Fisher Scientific, Inc., Shanghai, China). The mRNA sequencing Library Prep Kit for Illumina (NR601-01/02; Vazyme Biotech Co., Ltd., Nanjing, China) was used for RNA library construction, which was used according to the following manufacturer's steps: mRNA was screened using capture beads; the isolated mRNA was fragmented by Frag/Prime Buffer; cDNA was synthesized; adapters were connected to cDNA; fragments were sorted and amplified by PCR; and the size of the insert in the library was measured using the Agilent 2200 (Agilent Technologies, Inc., Guangzhou, China). All sequencing procidures were carried out using the Hi-Seq 2500 platform (Illumina Inc., San Diego, CA). Two independent samples (Cd treatment sample and control sample) on day 60 were used in this experiment. Each of the samples had four biology repeats.

Bioinformatics Analysis

Fast-QC (http://www.bioinformatics.babraham.ac.uk/projects/fastqc/) was used to analyze the raw data and filter away the low-quality sequences and adaptor sequences. Then, the remaining clean reads were mapped to the chicken genome using HISAT2 (version 2.1.0; https://daehwankimlab.github.io/hisat2/). The level of mRNA in the chicken heart was quantified as counts and FPKM, and the differentially expressed genes with a false discovery rate <0.05 and $|\log2 \text{ fold-change}|>1$

were identified using the DE-Seq2.0 algorithm. Functional analysis of these genes was performed using Gene Ontology (http://www.geneontology.org;), and pathway analysis was assessed using Kyoto Encyclopedia of Genes and Genomes (**KEGG**; http://www.genome.jp/kegg/). The sequencing data were submitted in the GenBank databases (https://www.ncbi.nlm.nih.gov/bioproject/PRJNA637406) under the accession number PRJNA637406.

Quantitative Real-Time PCR

Total RNA in the chicken heart was extracted using Trizol (15596026; Invitrogen, Thermo Fisher Scientific, Inc.), and the quantity was tested using the microspectrophotometer (OSE-260, TGem; TIANGEN, Beijing, China). cDNA was generated by reverse transcription of 1 μg of RNA using a reverse transcription kit (K1622; Thermo Fisher Scientific, Inc., Shanghai, China). The sequences of PCR primers (Table 2) were synthesized by Shanghai Sangon Biological (Shanghai, China). Quantitative real-time PCR analysis was carried out using the SYBR Green Master Mix (04913914001; Roche, Basel, Switzerland) and ABI Q6 (Applied Biosystems; Thermo Fisher Scientific, Inc., Shanghai, China) as per the following procedures: 95°C for 10 min, 45 cycles at 95°C for 15 s and at 60°C for 60 s. The internal control was GAPDH, and the relative expression level of mRNA was calculated using the comparative threshold cycle ($2^{-\Delta\Delta Cq}$) method (Livak and Schmittgen, 2001; Ibrahim et al., 2020). Two independent samples (Cd treatment sample, the control sample) on day 60 were used in this experiment. Each of the samples had four biology repeats.

Statistical Analysis

All date was expressed as mean ± SD in three duplicate experiments. The statistical analysis of oxidative stress–related molecules and mRNA in the chicken heart was carried out using the unpaired 2-tailed Student t test via SPSS 24.0 software (IBM Corp, Armonk, NY,). The statistically significant difference was considered at $P < 0.05$.

RESULTS

Cadmium-Triggered Oxidative Stress in the Chicken Heart

To evaluate the effect of Cd exposure on oxidative stress in the chicken heart, we examined the levels of oxidative stress–related markers (GSH, POD, SOD, and MDA). As shown in Figures 1A–1C, Cd treatment significantly decreased the concentration of nonenzymic antioxidant GSH and inhibited the activity of major detoxification enzymes POD and SOD at day 20, 40, and 60. Moreover, the lipid peroxidation level in the chicken heart, as evaluated using MDA levels, was markedly increased after exposure to Cd (Figure 1D), suggesting the oxidative stress response in the chicken heart may be stimulated by Cd.

Cadmium-Induced Histopathological Changes in the Chicken Heart

Previous studies demonstrated that oxidative stress was strongly related to organ damage (Myburgh et al., 2019). To investigate heart damage in chickens after exposure to Cd, H&E staining was performed to evaluate the Cd-induced histopathological changes in the chicken heart (Figure 2). In the Cd-induced chicken heart, we found that cardiomyocytes were arranged in disorder, cells were swelled and enlarged, and cardiomyocytes were partially necrotized. Cardiomyocytes showed a blurred morphological structure and notable inflammatory cell infiltration. But the heart of the chickens in the control group showed no obvious gross lesions. This result indicated that Cd exposure provoked heart damage in chickens, which is related to oxidative stress.

Analysis of Differentially Expressed Genes

Next, we performed high-throughput sequencing to investigate the differentially expressed genes involved in oxidative stress of the chicken heart. Approximately, 82 (control 1), 86 (control 2), 79 (control 3), and 80 (control 4) million high-quality clean reads in 4 control

Table 2. Primer sequences of mRNA for RT-qPCR.

Primer	Sequences (5′ to 3′)	Product expected length/bp	Tm/°C
GAPDH-F	GAAGGCTGGGGCTCATCTG	150	60
GAPDH-R	CAGTTGGTGGTGCACGATG		
DUSP8-F	CTGAAGGAGGATGGTACTTTGG	150	60
DUSP8-R	GCTTGTCCCTCAGTCTGATCT		
FGF7-F	AGCTTGCAATGACATGACTCC	74	60
FGF7-R	TTCTGGTATGTCGCTCAGGG		
ITGA11-F	CGGACCAGGCCTGATGTATT	81	60
ITGA11-R	ACAGCCAAGTCTATGAGCCC		
LAMA1-F	AACATGGCCCATCAGTCAGA	98	60
LAMA1-R	CATCAAATTGGCCTCGCTGA		
CREM-F	GAATTTCTCCACTGTCCATGC	157	60
CREM-R	TCCTTCTCAGCAAGTCATCTCT		

Abbreviation: RT-qPCR, quantitative real-time PCR.

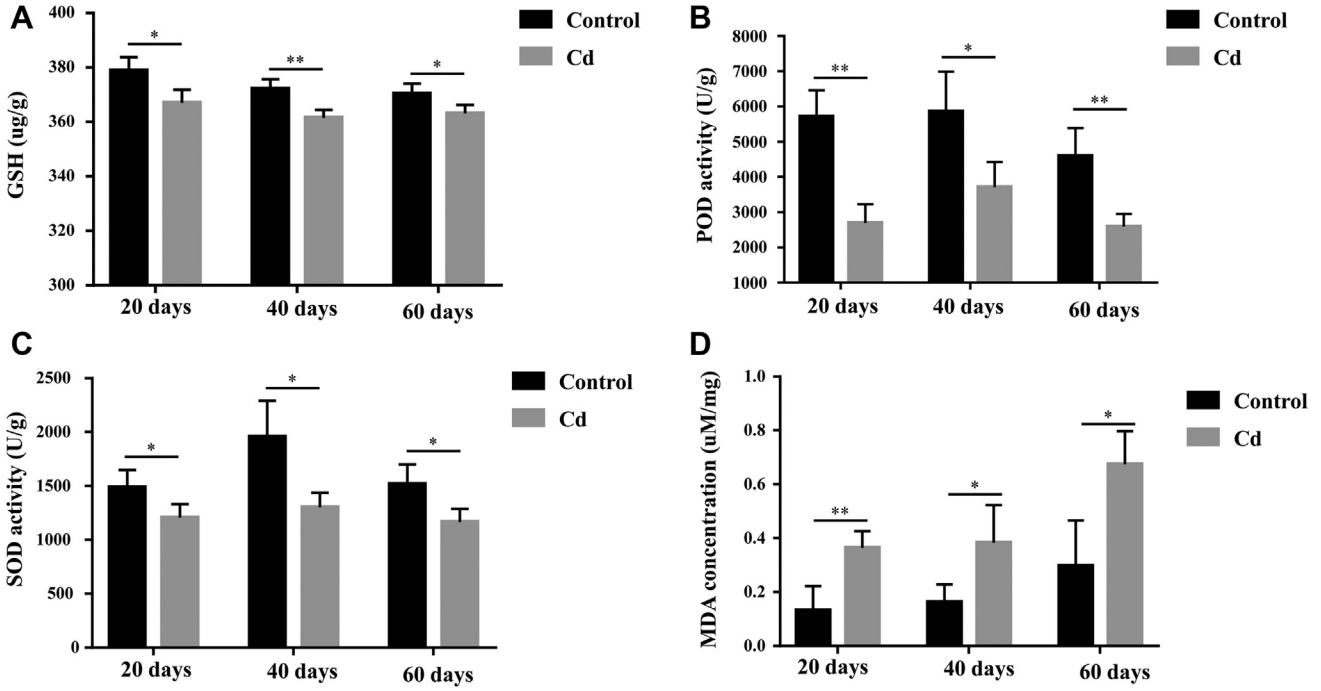

Figure 1. Cd-triggered oxidative stress in the chicken heart. (A) The expression level of GSH in chicken heart tissues subjected to cadmium chloride ($CdCl_2$, Cd) induction at day 20, 40, and 60. (B) The activity of POD was detected to evaluate the Cd-induced oxidative stress at day 20, 40, and 60. (C) The activity of SOD in chicken heart tissues was detected at day 20, 40, and 60. (D) MDA levels in the heart tissues of chickens induced by Cd at day 20, 40, and 60. Each experiment had two independent samples, including the cadmium treatment sample and the control sample, and each of the samples had five biology repeats. Each experiment was duplicated at least three times (unpaired 2-tailed Student t test; $^*P < 0.05$, $^{**}P < 0.01$). Abbreviations: Cd, cadmium; GSH, glutathione; MDA, malondialdehyde; POD, peroxidase; SOD, superoxide dismutase.

chickens were obtained, whereas clean reads in 4 Cd-induced chickens were 82 (Cd 1), 95 (Cd 2), 85 (Cd 3), and 92 (Cd 4) million, respectively, and 90.81 to 92.51% of clean reads in both the control and Cd-induced group were mapped to the reference genome (Table 3). Among these genes, we identified 34 differentially expressed mRNAs between the control group and Cd-induced group, which consisted of 23 upregulated and 11 downregulated genes in the Cd-induced group compared with the control group (Figure 3A). Hierarchical clustering of these differentially expressed genes was presented in Figure 3B, suggesting two major clusters (Cd-induced group and control group) were identified, and the Cd-induced group significantly differed from the control group.

Gene Ontology and KEGG Enrichment Analysis of Cd-Induced Differentially Expressed Genes

To understand the oxidative stress–related function of these differentially expressed genes induced by Cd, Gene Ontology and KEGG pathway analysis was conducted. Gene ontology term analysis (Figure 4A) showed that these genes were enriched in oxidative stress–related terms, including tissue development (Monteiro et al., 2017), negative regulation of cell differentiation (Chen et al., 2018) keratinocyte proliferation (Smirnov et al., 2016), and positive regulation of cell cycle (Baeeri et al., 2019). And the KEGG analysis determined that these differentially expressed genes were mostly enriched in pathways such as the transforming growth factor-beta signaling pathway, focal adhesion, the Wnt signaling pathway, regulation of the actin cytoskeleton, and the MAPK signaling pathway, which were implicated in oxidative stress (Farah et al., 2011; Lu et al., 2011;

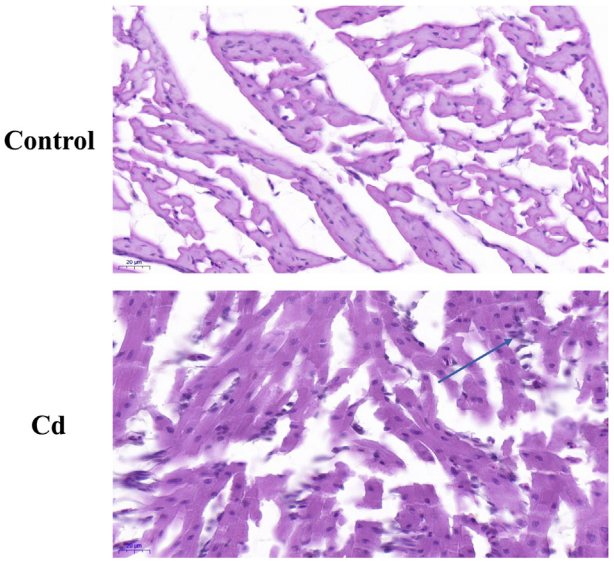

Figure 2. Cd-induced histopathological changes in the chicken heart. The histological structure of chicken heart tissues was observed by H&E staining. Magnification was 40×, and the scale bar was 20 μm. Inflammatory infiltration is shown by the blue arrow. Abbreviation: H&E, hematoxylin and eosin.

Table 3. Summary of the sequencing read alignment to the reference genome.

Type	All reads	Clean reads	Mapped reads	Mapped rate (%)
Control 1	87259646	82544264	74975953	90.83
Control 2	90507786	86240344	78316529	90.81
Control 3	82937082	79109680	72577847	91.74
Control 4	84438582	79917896	73269207	91.68
Cd 1	86810662	82225048	74794818	90.96
Cd 2	99682764	95431100	87908874	92.11
Cd 3	88993962	85430122	78900971	92.36
Cd 4	96735732	92674106	85737459	92.51

Abbreviation: Cd, cadmium.

Lou et al., 2018; Zhang et al., 2018b; Kim et al., 2020) (Figure 4B).

Quantitative Real-Time PCR Validated the Expression Patterns of Candidate Genes Involved in Oxidative Stress

Next, we selected five genes (CREM, DUSP8, FGF7, ITGA11, and LAMA1) for further study, which possessed the characteristics of abundant expression, higher significance, and higher fold change. Subsequently, RT-qPCR was used to verify the expression of candidate mRNAs in chicken heart tissues. When compared with the control group, we found that CREM, DUSP8, FGF7, and ITGA11 were significantly downregulated, whereas LAMA1 was upregulated in the Cd-induced group (Figure 5A). Obviously, the RT-qPCR results of CREM, DUSP8, ITGA11, and LAMA1 were basically consistent with the RNA sequencing (**RNA-seq**) data, while the changes of FGF7 in chicken heart tissues detected by RT-qPCR were not in conformity with those detected by RNA-seq (Figure 5B).

DISCUSSION

As a nondegradable heavy metal, Cd is a widely environmental pollutant and results in high toxicity to various organs of the human body and animals (Irfan et al., 2013). However, the effect and underlying molecular mechanism of Cd toxicity in the chicken heart are not clearly known. At present, our study demonstrated that Cd could trigger oxidative stress and then lead to heart damage in chickens. The whole-transcriptome RNA-Seq identified 23 upregulated genes and 11 downregulated genes in the Cd-

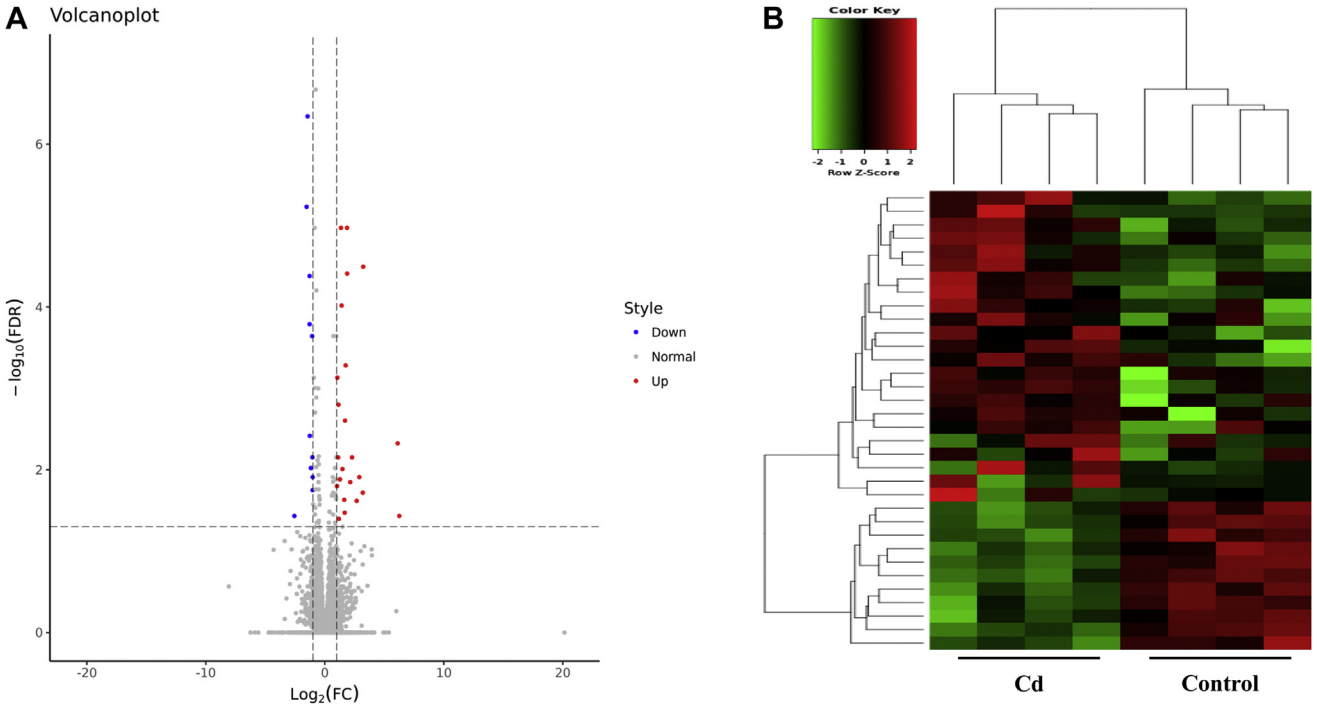

Figure 3. Analysis of differentially expressed genes. (A) Volcano plot of differentially expressed genes in heart tissues of the Cd-induced group and control group. The x-axis and y-axis indicates $\log_2$ (fold change) and $-\log_{10}$ (FDR) of differentially expressed genes in heart tissues, respectively. The red color represents upregulated genes, and the blue color represents downregulated genes. (B) Clustering map of differentially expression genes in heart tissues between the Cd-induced group and control group. Green to red color displays low to high expression levels, respectively. Abbreviations: Cd, cadmium; FDR, false discovery rate.

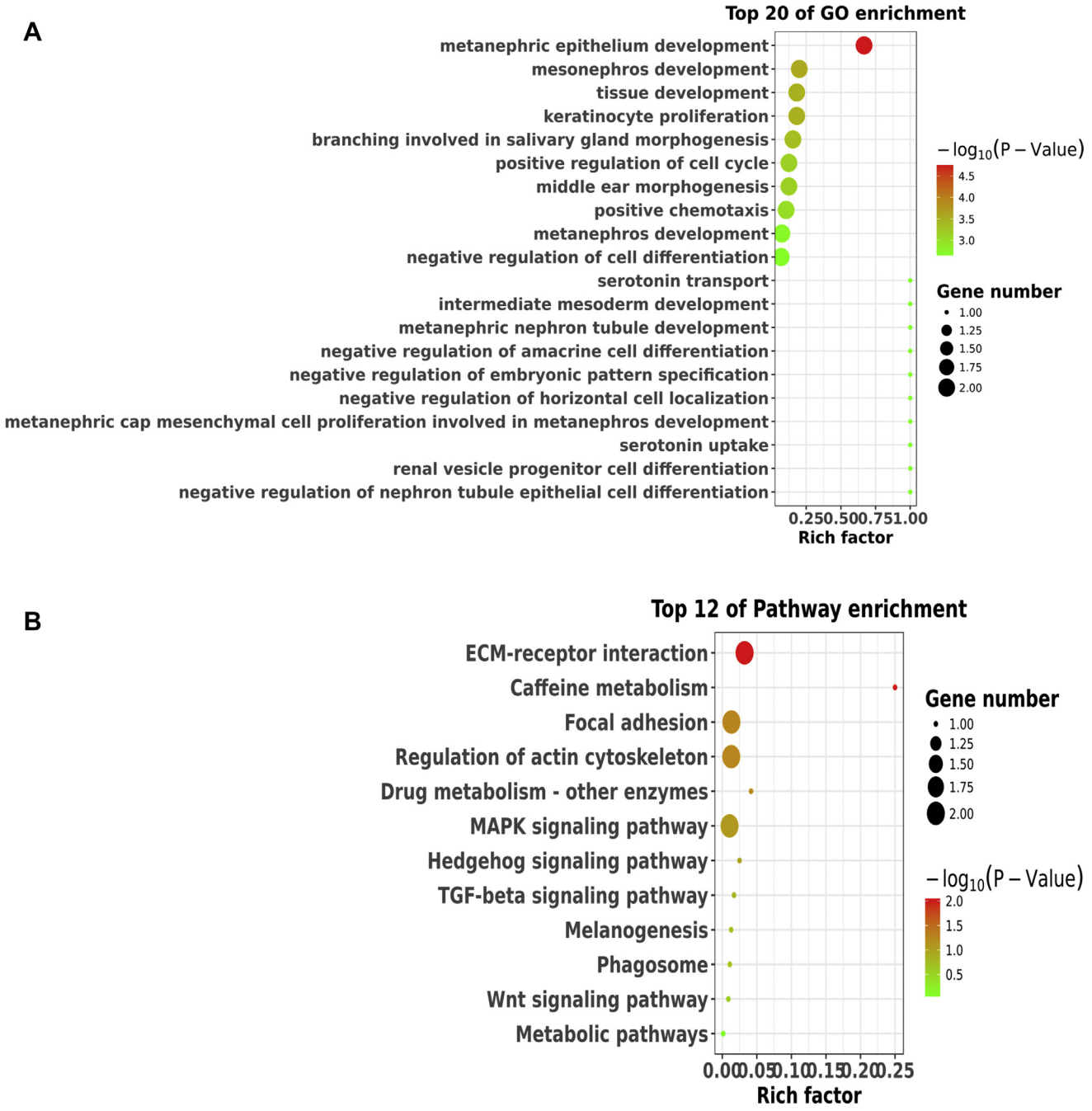

Figure 4. GO and KEGG enrichment analysis of Cd-induced differentially expressed genes. (A) Top 20 enriched GO terms of 34 differentially expressed genes in the Cd-induced group compared with the control group. (B) Top 12 enriched KEGG terms of 34 differentially expressed genes in the Cd-induced group compared with the control group. Abbreviations: ECM, extracellular matrix; GO, Gene Ontology; KEGG, Kyoto Encyclopedia of Genes and Genomes; MAPK, mitogen-activated protein kinase; TGF, transforming growth factor.

induced chicken heart relative to those in the control group, which were involved in oxidative stress–related signaling pathways, such as the transforming growth factor-beta signaling pathway, focal adhesion, the Wnt signaling pathway, regulation of the actin cytoskeleton, and the MAPK signaling pathway. Quantitative real-time PCR analysis indicated that CREM, DUSP8, FGF7, and ITGA11 expression was markedly decreased by Cd induction, whereas LAMA1 expression was increased.

One of the main mechanisms of Cd-induced multiorgan toxicity is oxidative stress (de Boer et al., 2011). Substantial studies have shown that oxidative stress was involved in cardiac injury. Oxidative stress–mediated cardiomyocyte damage blunted the protection against ischemia-reperfusion injury (Babiker et al., 2018), and the decline in oxidative stress was correlated with less severe lesions in hearts of rats receiving thymoquinone treatment (de Andrade et al., 2017). What is more, the myocardial ischemia-reperfusion (I/R) injury was alleviated by PGI2 via decreased oxidative stress (Zhong et al., 2019), and heart protection by NGR1 was closely related to inhibition of oxidative stress (Yu et al., 2016). It is reported that oxidative stress could be

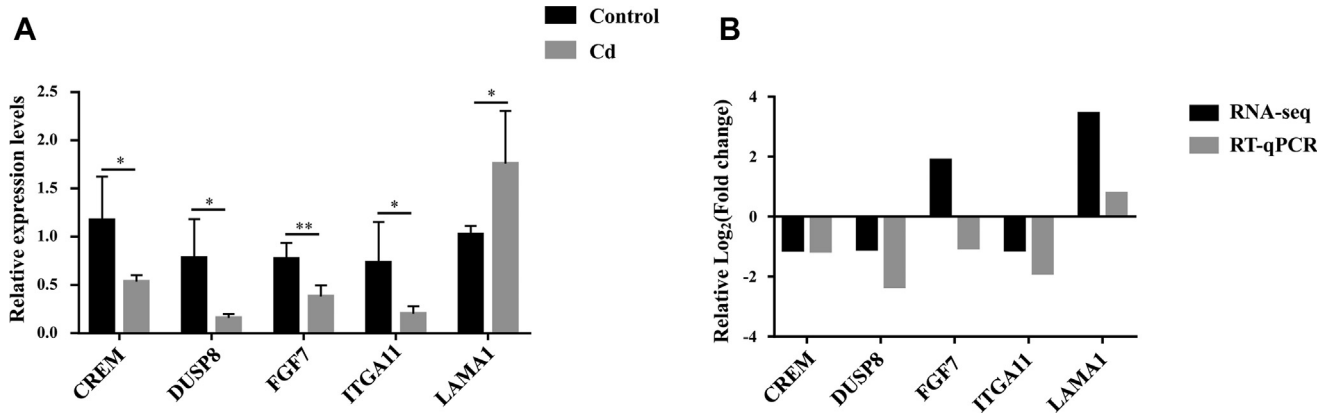

Figure 5. RT-qPCR validated the expression patterns of candidate genes involved in oxidative stress. (A) The relative expression of five screened genes in the chicken heart was detected by RT-qPCR. The expression of genes was measured by the $2^{-\Delta\Delta Cq}$ method. Each experiment was duplicated at least three times. (B) The comparison of expression levels of candidate genes as per RNA-seq and RT-qPCR analysis. Each experiment had two independent samples, including the cadmium treatment sample and the control sample, and each of the samples had four biology repeats (unpaired 2-tailed Student t test; $^{*}P < 0.05$, $^{**}P < 0.01$). Abbreviations: RNA-seq, RNA sequencing; RT-qPCR, quantitative real-time PCR; Cq, comparative threshold.

induced by ingestion of excessive Cd (Meng et al., 2017), and oxidative stress was related to Cd-induced toxicity in both in vivo or in vitro studies (Yu et al., 2008). Similarly, our results showed that the activation of major detoxification enzymes POD and SOD and the level of GSH were decreased in the Cd-induced chicken heart. Malondialdehyde, a main marker of oxidative stress, was accumulated in the heart of chickens exposed to Cd. Together, these findings suggested that cardiac injury in Cd-induced chickens was implicated in increased oxidative stress.

To explore the most critical molecules and pathways, RNA-seq and RT-qPCR was performed, and the dysregulated genes in the Cd-induced chicken heart were identified. CREM, DUSP8, ITGA11, and LAMA1 were the most dysregulated genes in the Cd-induced chicken heart. Several findings demonstrated that these 4 genes participated in oxidative stress. CREM mRNA is remarkably expressed in the human myocardium and plays pivotal roles in the adrenergic signaling pathway, which was involved in oxidative stress (Isoda et al., 2003; Aldaba-Muruato et al., 2017). DUSP8 is a member of dual-specificity phosphatases that can be phosphorylated in response to arsenite-induced oxidative stress (Karkali and Panayotou, 2012). Pathway analysis indicated that DUSP8 was involved in the MAPK signaling pathway, which was activated by Cd via induction of reactive oxygen species (Chen et al., 2008). Previous studies and KEGG analysis demonstrated that ITGA11 and LAMA1 were associated with the PI3K/Akt signaling pathway (Ryu and Lee, 2017). Cadmium triggered apoptosis in the chicken kidney via the activity of the PI3K/AKT signaling pathway (Bao et al., 2017), catestatin protected against oxidative stress–induced apoptosis in the ischemic–reperfused myocardium, and hypoxia/reoxygenation-induced oxidative stress in cardiomyocytes was attenuated by the PI3K/Akt signaling pathway (Li et al., 2017; Chu et al., 2019). Our study showed the expression of CREM, DUSP8, and ITGA11 was markedly reduced, whereas LAMA1 expression was induced in the chicken heart subjected to Cd treatment, suggesting that Cd may induce oxidative stress by regulating CREM, DUSP8, ITGA11, and LAMA1.

In conclusion, this study indicated that Cd induced oxidative stress and led to cardiac damage in the heart of chickens, the expression patterns of mRNAs involved in oxidative stress in the Cd-induced chicken heart were constructed, and CREM, DUSP8, and ITGA11 were downregulated by Cd treatment, whereas LAMA1 was upregulated. All these references for further study of Cd toxicity–induced heart dysfunction may be helpful to pinpoint the underlying molecular mechanism of Cd toxicity in chickens. Transcriptome sequencing will help to elucidate the Cd-induced oxidative stress from a new perspective.

ACKNOWLEDGMENTS

This work was supported by National Modern Agricultural Industrial Technology System Construction Project (CARS-41-G04), Science and Technology Research and Development Project of Sichuan Province (20SYSX0175), Sichuan Provincial 13th Five-year Breeding Program (2016NYZ0043), and Major Science and Technology Projects of Sichuan Province (2018NZDZX0004). All treatment procedures were approved by the Institutional Animal Care and Use Committee of Sichuan Animal Science Academy.

Availability of data and materials: The data sets used and/or analyzed during the present study are available from the corresponding author on reasonable request.

DISCLOSURES

The authors declare that they have no known competing financial interests or personal relationships that could have appeared to influence the work reported in this paper.

SUPPLEMENTARY DATA

Supplementary data associated with this article can be found in the online version at https://doi.org/10.1016/j.psj.2020.12.029.

REFERENCES

Aldaba-Muruato, L. R., M. H. Muñoz-Ortega, J. R. Macías-Pérez, J. Pulido-Ortega, S. L. Martínez-Hernández, and J. Ventura-Juárez. 2017. Adrenergic regulation during acute hepatic infection with Entamoeba histolytica in the hamster: involvement of oxidative stress, Nrf2 and NF-KappaB. Parasite 24:46.

Babiker, F., A. Al-Kouh, and N. Kilarkaje. 2018. Lead exposure induces oxidative stress, apoptosis, and attenuates protection of cardiac myocytes against ischemia-reperfusion injury. Drug Chem. Toxicol. 42:1–10.

Baeeri, M., H. Bahadar, M. Rahimifard, M. Navaei-Nigjeh, R. Khorasani, M. A. Rezvanfar, M. Gholami, and M. Abdollahi. 2019. α-Lipoic acid prevents senescence, cell cycle arrest, and inflammatory cues in fibroblasts by inhibiting oxidative stress. Pharmacol. Res. 141:214–223.

Bao, R. K., S. F. Zheng, and X. Y. Wang. 2017. Selenium protects against cadmium-induced kidney apoptosis in chickens by activating the PI3K/AKT/Bcl-2 signaling pathway. Environ. Sci. Pollut. Res. Int. 24:20342–20353.

Chen, L., L. Liu, and S. Huang. 2008. Cadmium activates the mitogen-activated protein kinase (MAPK) pathway via induction of reactive oxygen species and inhibition of protein phosphatases 2A and 5. Free Radic. Biol. Med. 45:1035–1044.

Chen, X., W. B. Shen, P. Yang, D. Dong, W. Sun, and P. Yang. 2018. High glucose inhibits neural stem cell differentiation through oxidative stress and endoplasmic reticulum stress. Stem Cells Dev 27:745–755.

Chu, S. Y., F. Peng, J. Wang, L. Liu, L. Meng, J. Zhao, X. N. Han, and W. H. Ding. 2019. Catestatin in defense of oxidative-stress-induced apoptosis: a novel mechanism by activating the beta2 adrenergic receptor and PKB/Akt pathway in ischemic-reperfused myocardium. Peptides 123:170200.

de Andrade, T. U., G. A. Brasil, D. C. Endringer, F. R. da Nóbrega, and D. P. de Sousa. 2017. Cardiovascular activity of the chemical Constituents of essential Oils. Molecules (Basel, Switzerland) 22:1539.

de Boer, M. E., S. Berg, M. J. T. N. Timmermans, J. T. den Dunnen, N. M. van Straalen, J. Ellers, and D. Roelofs. 2011. High throughput nano-liter RT-qPCR to classify soil contamination using a soil arthropod. BMC Mol. Biol. 12:11.

Ezedom, T., and S. O. Asagba. 2016. Effect of a controlled food-chain mediated exposure to cadmium and arsenic on oxidative enzymes in the tissues of rats. Toxicol. Reports 3:708–715.

Farah, M. E., V. Sirotkin, B. Haarer, D. Kakhniashvili, and D. C. Amberg. 2011. Diverse protective roles of the actin cytoskeleton during oxidative stress. Cytoskeleton (Hoboken) 68:340–354.

Ge, J., C. Zhang, Y. C. Sun, Q. Zhang, M. W. Lv, K. Guo, and J. L. Li. 2019. Cadmium exposure triggers mitochondrial dysfunction and oxidative stress in chicken (Gallus gallus) kidney via mitochondrial UPR inhibition and Nrf2-mediated antioxidant defense activation. Sci. Total Environ. 689:1160–1171.

Guo, K., J. Ge, C. Zhang, M. W. Lv, Q. Zhang, M. Talukder, and J. L. Li. 2020. `Cadmium induced cardiac inflammation in chicken (Gallus gallus) via modulating cytochrome P450 systems and Nrf2 mediated antioxidant defense. Chemosphere 249:125858.

Hu, X., R. Zhang, Y. Xie, H. Wang, and M. Ge. 2017. The protective effects of Polysaccharides from Agaricus blazei Murill against cadmium-induced oxidant stress and inflammatory damage in chicken livers. Biol. Trace Elem. Res. 178:117–126.

Ibrahim, K., N. A. Abdul Murad, R. Harun, and R. Jamal. 2020. Knockdown of Tousled-like kinase 1 inhibits survival of glioblastoma multiforme cells. Int. J. Mol. Med. 46:685–699.

Irfan, M., S. Hayat, A. Ahmad, and M. N. Alyemeni. 2013. Soil cadmium enrichment: Allocation and plant physiological manifestations. Saudi. J. Biol. Sci. 20:1–10.

Isoda, T., N. Paolocci, K. Haghighi, C. Wang, Y. Wang, D. Georgakopoulos, G. Servillo, M. A. Della Fazia, E. G. Kranias, A. A. Depaoli-Roach, P. Sassone-Corsi, and D. A. Kass. 2003. Novel regulation of cardiac force-frequency relation by CREM (cAMP response element modulator). Faseb. J. 17:144–151.

Karkali, K., and G. Panayotou. 2012. The Drosophila DUSP puckered is phosphorylated by JNK and p38 in response to arsenite-induced oxidative stress. Biochem. Biophys. Res. Commun. 418:301–306.

Kim, S. J., M. J. Shin, D. W. Kim, H. J. Yeo, E. J. Yeo, Y. J. Choi, E. J. Sohn, K. H. Han, J. Park, K. W. Lee, and J. K. Park. 2020. *Tat-Biliverdin Reductase A Exerts a Protective Role in Oxidative Stress-Induced Hippocampal Neuronal Cell Damage by Regulating the Apoptosis and MAPK Signaling*. Int J Mol Sci. 21:2672.

Kubier, A., R. T. Wilkin, and T. Pichler. 2019. Cadmium in soils and groundwater: a review. Appl. Geochem 108:1–16.

Li, L., Y. Zhou, Y. Li, L. Wang, L. Sun, L. Zhou, H. Arai, Y. Qi, and Y. Xu. 2017. Aqueous extract of Cortex Dictamni protects H9c2 cardiomyocytes from hypoxia/reoxygenation-induced oxidative stress and apoptosis by PI3K/Akt signaling pathway. Biomed. Pharmacother. 89:233–244.

Liu, S., F. Xu, J. Fu, and S. Li. 2015. Protective roles of selenium on Nitric Oxide and the gene expression of inflammatory Cytokines induced by cadmium in chicken Splenic Lymphocytes. Biol. Trace Elem. Res. 168:252–260.

Livak, K. J., and T. D. Schmittgen. 2001. Analysis of relative gene expression data using real-time quantitative PCR and the 2(-Delta Delta C(T)) Method. Methods 25:402–408.

Lou, Z., A. P. Wang, X. M. Duan, G. H. Hu, G. L. Song, M. L. Zuo, and Z. B. Yang. 2018. Upregulation of NOX2 and NOX4 mediated by TGF-β signaling pathway Exacerbates Cerebral ischemia/reperfusion oxidative stress injury. Cell. Physiol. Biochem. 46:2103–2113.

Lu, Q., P. Sakhatskyy, K. Grinnell, J. Newton, M. Ortiz, Y. Wang, J. Sanchez-Esteban, E. O. Harrington, and S. Rounds. 2011. Cigarette smoke causes lung vascular barrier dysfunction via oxidative stress-mediated inhibition of RhoA and focal adhesion kinase. Am. J. Physiol. Lung Cell Mol. Physiol. 301:L847–L857.

Meng, J., W. Wang, L. Li, Q. Yin, and G. Zhang. 2017. Cadmium effects on DNA and protein metabolism in oyster (Crassostrea gigas) revealed by proteomic analyses. Scientific Reports 7:11716.

Monteiro, H. P., F. T. Ogata, and A. Stern. 2017. Thioredoxin promotes survival signaling events under nitrosative/oxidative stress associated with cancer development. Biomed. J. 40:189–199.

Myburgh, C., H. W. Huisman, and C. M. C. Mels. 2019. Three-year change in oxidative stress markers is linked to target organ damage in black and white men: the SABPA study. Hypertens. Res. 42:1961–1970.

Nouri, M., and A. Haddioui. 2016. Human and animal health risk assessment of metal contamination in soil and plants from Ait Ammar abandoned iron mine, Morocco. Environ. Monit. Assess. 188:6.

Ryu, D., and C. Lee. 2017. Expression quantitative trait loci for PI3K/AKT pathway. Medicine 96:e5817.

Smirnov, A., E. Panatta, A. Lena, D. Castiglia, N. Di Daniele, G. Melino, and E. Candi. 2016. FOXM1 regulates proliferation, senescence and oxidative stress in keratinocytes and cancer cells. Aging. 8:1384–1397.

Tang, K. K., H. Q. Li, K. C. Qu, and R. F. Fan. 2019. Selenium alleviates cadmium-induced inflammation and meat quality degradation via antioxidant and anti-inflammation in chicken breast muscles. Environ. Sci. Pollut. Res. Int. 26:23453–23459.

Teng, X., W. Zhang, Y. Song, H. Wang, M. Ge, and R. Zhang. 2019. Protective effects of Ganoderma lucidum triterpenoids on oxidative stress and apoptosis in the spleen of chickens induced by cadmium. Environ. Sci. Poll. Res. Int 26:23967–23980.

Wang, X., R. Bao, and J. Fu. 2017. The Antagonistic effect of selenium on cadmium-induced damage and mRNA levels of Selenoprotein genes and inflammatory factors in chicken kidney tissue. Biol. Trace Elem. Res. 181:331–339.

Wang, S. H., Y. L. Shih, W. C. Ko, Y. H. Wei, and C. M. Shih. 2008. Cadmium-induced autophagy and apoptosis are mediated by a calcium signaling pathway. Cell. Mol. Life Sci. 65:3640–3652.

Xiong, X., Y. Zhang, H. Xing, and S. Xu. 2019. Ameliorative effect of Selenomethionine on cadmium-induced hepatocyte apoptosis via regulating PI3K/AKT pathway in chickens. Biol. Trace Elem. Res. 195:559–568.

Xu, Z., X. Jin, T. Pan, T. Liu, N. Wan, and S. Li. 2017. Antagonistic effects of selenium on cadmium-induced apoptosis by restoring the mitochondrial dynamic equilibrium and energy metabolism in chicken spleens. Oncotarget 8:52629–52641.

Yu, C., C. Yang, X. Song, J. Li, H. Peng, M. Qiu, L. Yang, H. Du, X. Jiang, and Y. Liu. 2020. Long non-coding RNA expression profile in broiler liver with cadmium-induced oxidative damage. Biol. Trace Elem. Res. 1:1–19.

Yu, X., S. Hong, and E. M. Faustman. 2008. Cadmium-induced activation of stress signaling pathways, disruption of ubiquitin-dependent protein degradation and apoptosis in primary rat Sertoli cell-gonocyte cocultures. Toxicol. Sci. 104:385–396.

Yu, Y., G. Sun, Y. Luo, M. Wang, R. Chen, J. Zhang, Q. Ai, N. Xing, and X. Sun. 2016. Cardioprotective effects of Notoginsenoside R1 against ischemia/reperfusion injuries by regulating oxidative stress- and endoplasmic reticulum stress- related signaling pathways. Sci. Rep. 6:21730.

Zhang, L., Y. Fang, X. Cheng, Y. J. Lian, and H. L. Xu. 2018b. Silencing of long Noncoding RNA SOX21-AS1 Relieves Neuronal oxidative stress injury in Mice with Alzheimer's disease by Upregulating FZD3/5 via the Wnt signaling pathway. Mol. Neurobiol. 56:3522–3537.

Zhang, D., Y. Li, T. Zhang, J. Liu, A. R. Jahejo, L. Yang, P. Chen, G. Ning, N. Huo, H. Ma, F. Yan, and W. Tian. 2018a. Protective effects of zinc and N-acetyl-L-cysteine supplementation against cadmium induced erythrocyte cytotoxicity in Arbor Acres broiler chickens (Gallus gallus domesticus). Ecotoxicol. Environ. Saf. 163:331–339.

Zhong, B., S. Ma, and D. H. Wang. 2019. Protease-activated receptor 2 protects against myocardial ischemia-reperfusion injury through the lipoxygenase pathway and TRPV1 channels. Exp. Therapeutic Medicine 18:3636–3642.

Zhang, Z., Z. Zheng, J. Cai, Q. Liu, J. Yang, Y. Gong, M. Wu, Q. Shen, and S. Xu. 2017. Effect of cadmium on oxidative stress and immune function of common carp (Cyprinus carpio L.) by transcriptome analysis. Aquat. Toxicol. 192:171–177.